Genetic Algorithm-Based Optimization of Feedback Control Scheme for Wall Turbulence

Kenichi MORIMOTO, Kaoru IWAMOTO, Yuji SUZUKI, and Nobuhide KASAGI
Department of Mechanical Engineering, The University of Tokyo,
Hongo 7-3-1, Bunkyo-ku, Tokyo 113-8656, Japan
phone: +81 03 5841 6419, Fax: +81 03 5800 6999, E-mail: morimoto@thtlab.t.u-tokyo.ac.jp

Although various feedback control algorithms are proposed for wall turbulence, most efficient control schemes require the spanwise wall shear stress, which is difficult to measure in physical experiments. In the present study, a new control scheme based on the streamwise wall shear stress is developed with the aid of genetic algorithms. Local blowing/suction at the wall was employed as the control input, and its distribution was optimized in order to minimize the wall skin friction. It is found through direct numerical simulation of turbulent channel flow that about 12% drag reduction is obtained by using a control scheme, which gives asymmetric distribution of the control input in the spanwise direction. The control input becomes out of phase with the vortices because of the drastic change of the streaky structures in the vicinity of the wall.

1. INTRODUCTION

In the past several decades, numerous studies have been carried out in order to control turbulent flow and its concomitant transport phenomena such as friction drag and heat transfer, but most attempts employ time-independent/spatially-uniform control methodologies. Recent development of microelectromechanical system (MEMS) technology enables us to fabricate prototypes of micro sensors and actuators, which can offer localized time-dependent control input depending on instantaneous flow condition.

Among various control strategies, active feedback control is of great concern because of its potential to manipulate turbulent flows with relatively small energy input (Moin & Bewley, 1994; Gad-el-Hak, 1996; Kasagi, 1998). Choi *et al*. (1994) employed local blowing/suction at the wall, which is based on the wall-normal velocity at $y^+ = 10$, and they obtained about 25% drag reduction in their direct numerical simulation (DNS) of turbulent channel flow. Bewley *et al*. (1993) applied a suboptimal control theory to turbulent channel flow, and obtained about 17% drag reduction. Recently, Lee *et al*. (1998) proposed a new suboptimal control algorithm based only on the wall variables such as the spanwise wall shear stress and the wall pressure fluctuations. Moreover, Lee *et al*. (1997) employed neural networks (NNs) to predict the wall-normal velocity at a prescribed elevation from the spanwise wall shear stress, and they obtained about 20% drag reduction in their DNS of turbulent channel flow. In these studies, however, quantities such as the spanwise wall shear stress and the wall pressure are required for sensing information, which are difficult to measure in practical flow systems.

The objective of the present study is to develop a new control algorithm based only on the streamwise wall shear stress and evaluate its performance with DNS of turbulent channel flow. In the present study, local blowing/suction on the wall is employed as control input, and its distribution is optimized in order to minimize the time-averaged wall skin friction with the aid of genetic algorithms (GAs). Optimal control is already applied to wall turbulence by Bewley *et al*. (2001), but GA-based schemes have the potential to provide different control scheme with a much simpler form.

2. GENETIC ALGORITHM (GA)

Among four categories of control strategies (Gad-el-Hak, 1996), GA-based control algorithm is grouped into the adaptive scheme, in which control parameters are optimized through a training process with/without desired response of the controller. Once the control parameters are determined, the control input is readily calculated using algebraic equations. Therefore, GA-based control systems have an advantage in small computational load, since time lag between sensing and actuation is crucial for stability of control systems. In a separate work, the authors' group is developing a field programmable gate array (FPGA) controller, which enables us to employ the present GA-based scheme in laboratory experiment in a wind tunnel.

Genetic algorithm, which was derived from the evolution process of animals and plants, is one of the optimization methods with random search (e.g., Goldberg, 1989). Basically, GA consists of three kinds of genetic operations: selection, crossover and mutation. Genes are evolved through these operations so as to maximize/minimize the prescribed cost function, and the optimal solution is found as a result of successive generations. GA attracts much attention because of its applicability to various kinds of optimization problems.

Figure 1 shows a schematic diagram of GA-based control. Control parameters to be optimized are transformed into genes, and N individuals including a set of genes are made. DNS using each individual is independently made and the cost function is calculated. Then, the individual having smaller cost is statistically selected as parents, and two offsprings are made through crossover operation between them. In total, N children are created by applying the crossover operation $N/2$ times. Finally, mutations at a given rate are applied to all genes of the N individuals. New generations are successively produced by repeating this procedure, and the optimal solution is obtained when the evolution is found to be in convergence. In the present study, the cost function is set to be the wall skin friction averaged over a time period of 100 viscous time units.

3. NUMERICAL PROCEDURES AND CONTROL METHODS

The numerical technique used in this study is almost the same as that of Kim *et al.*(1987); a pseudo-spectral method with Fourier series was employed in the streamwise (x-) and spanwise (z-) directions, while a Chebyshev polynomial expansion was used in the wall-normal (y-) direction. A fourth-order Runge-Kutta scheme and a second-order Crank-Nicolson scheme are used for time discretization of the nonlinear terms and the viscous terms, respectively. The Reynolds number Re_τ, based on the wall friction velocity u_τ and the channel half-width δ, is 100, and the flow rate was kept constant. In order to reduce the computational load during optimization procedure using GA, the size of the computational domain is $1.25\pi\delta \times 2\delta \times 0.5\pi\delta$ in the x-, y-, and z- directions, respectively (hereafter, Domain I), using $16 \times 65 \times 16$ spectral modes (in the x-, y-, and z- directions, respectively). When optimized control scheme is obtained, the computational domain is expanded into $5\pi\delta \times 2\delta \times 2\pi\delta$ (hereafter, Domain II), using $64 \times 65 \times 64$ spectral modes in order to evaluate its performance. Hereafter, u, v, and w denote the velocity components in the x- , y-, and z- directions, respectively. The subscript w represents the value at the wall, and the superscript + represents a quantity non-dimensionalized by u_τ and the kinematic viscosity ν. A fully developed flow field is used as the initial condition. During the optimization process, the instantaneous flow field of the unmanipulated channel in the previous generation is chosen as the initial flow field in the next generation in order not to be trapped in local minima.

In the present study, wall blowing/suction in physical space is assumed to be the weighted summation of the streamwise wall shear stresses measured with virtual sensors aligned in the spanwise direction as follows:

$$v_w^+\left(x^+, z^+\right) = C\left(\sum_{n=-m}^{m} W_n \tau_w^+\left(x^+, z^+ + n\Delta z^+\right)\right) - \ll v_w^+ \gg, \quad \tau_w^+ = \left.\frac{\partial u^+}{\partial y^+}\right|_w, \tag{1}$$

where W_n denote weights to be optimized, and $(2m+1)$ is the total number of the weights. The spanwise spacing between the virtual sensors Δz^+ is 6.5, which is the minimal grid spacing in the spanwise direction. The second term of the RHS of Eq. (1) denotes an ensemble average of v_w^+, which ensures the total sum of v_w^+ being zero at each time step, although its contribution is negligible.

Each W_n ($-1 < W_n < 1$) is expressed as a binary-coded string with 8 bits, and the weight distribution is determined through the optimization process described in Chap. 2. In the present study, mutation rate is set to be 0.05.

For evaluating the control effect under constant energy input, the constant C in Eq. (1) is separately determined at each time step in such a way that the root-mean-square (rms) value of v_w^+ is 0.15, which is almost the same as the rms value of v^+ at $y^+ = 10$ in the unmanipulated channel.

4. RESULTS AND DISCUSSION

4.1 Weight Distribution

In order to obtain convergent solutions efficiently, two modes for W_n are defined as follows:

$$\begin{cases} W_0 = 0, \quad W_{-n} = -W_n \ \ (n = 1,2,3) \\ 0 \le W_1 \le 1, \quad -1 \le W_n \le 1 \ \ (n = 2,3) \end{cases} \quad \text{(Mode 1)}, \tag{2}$$

$$\begin{cases} W_{-n} = W_n \\ -1 \le W_n \le 1 \end{cases} \ (n = 0,1,2,3) \quad \text{(Mode 2)}, \tag{3}$$

where Mode 1 and 2 are respectively antisymmetric and symmetric weight distributions in the spanwise direction. In the present study, m in Eq. (1) is set to be 3, so that the spanwise extent of the sensor array is about 40 (ν/u_τ), which is slightly smaller than half the mean spacing of streaks.

Figure 2 shows the evolution of the maximum drag reduction rate. The drag reduction of about 11% and 8.5% is achieved in Mode 1 and 2, respectively. The number of generations G, which is required for the solution to be convergent, is 97 and 171. The population size N, that is, the number of individuals evaluated at each generation, is 60 and 30, respectively, so that the total number of DNSs until the convergent solution is obtained, $G \times N$, is 5000 ~ 6000 for both modes. Since larger drag reduction is obtained in Mode 1 than in Mode 2, the discussion hereafter is focused on the result of Mode 1.

Figure 3 shows the weight distribution optimized, where W_n at $\Delta z^+ = \pm 19.5$ have large absolute values, while others in the range of $-13 < \Delta z^+ < 13$ are almost zero. Therefore, the control input is almost proportional to the spanwise differential of the streamwise wall shear stresses about ± 20 (ν/u_τ) apart in the spanwise direction from actuators. From this result, the most efficient control input can be written in the following simple form (in physical space):

$$v_w = C\left\{\tau_w\left(x^+, z^+ + 20\right) - \tau_w\left(x^+, z^+ - 20\right)\right\}. \tag{4}$$

The Fourier representation of Eq. (4) is

$$\widehat{v_w}\left(k_x, k_z\right) = C\left\{i \sin\left(\frac{k_z}{16}\pi\right)\right\} \cdot \widehat{\tau_w}\left(k_x, k_z\right), \tag{5}$$

where the hat denotes the Fourier coefficient, and k_x and k_z denote the streamwise and spanwise wave numbers in the x- and z- directions, respectively. From Eq. (5), one can expect that the phase of v_w is $\pi/2$ ahead of that of τ_w regardless of k_x or k_z , and the magnitude of v_w is the most sensitive to τ_w when k_z equals to 8. Note that the wavelength of the wave of $k_z = 8$ corresponds to about 80 (ν/u_τ) in the physical space, which is close to the spacing of the streaky structures most frequently observed.

4.2 Control Effect and Drag Reduction Mechanism

We applied the control scheme given in Eq. (4) to a larger computational domain (Domain II) in order to evaluate its efficiency and examine its effect on turbulent structures. Figure 4 shows the time histories of the pressure gradients normalized by the time-averaged pressure gradient of the unmanipulated channel. The skin friction decreases drastically as soon as the control starts, and the maximum drag reduction rate of about 18% is obtained. The mean drag reduction rate during the period $t^+ = 0 \sim 2500$ is about 12%. The rms velocity fluctuations in wall coordinates are shown in Fig. 5. As is often observed in drag-reduced channels, turbulent intensities are significantly reduced by the control.

It is now clear that we could obtain significant drag reduction by the present control scheme having asymmetric distribution of the control input in the spanwise direction as shown in Fig. 3. In order to investigate the present drag reduction mechanism, we examined the relationship between control input v_w and near-wall streamwise vortices, which play a dominant role in high skin friction region in wall turbulence (e.g., Robinson, 1991; Kasagi *et al*., 1995).

To do this, we employ conditional averaging method using the second invariant of the deformation tensor ($Q^+ < -0.01$) at $y^+ = 14.3$, and extract flow structure around the near-wall streamwise vortices. The instantaneous flow field surrounding the detection points are spatially-averaged depending also on the sign of the streamwise vorticity. Figure 6 shows conditionally-averaged flow field with $\omega_x < 0$. Figure 6 (a) shows the flow field just after the onset of control ($t^+ = 2.5$), where the flow field should not be affected by the control input yet. As can be conjectured from Eq. (4), the control input becomes largest at the boundary between high and low speed regions, which is located beneath streamwise vortices; blowing is applied against the vortices with $\omega_x > 0$, while suction is applied against the vortices with $\omega_x < 0$. If this type of control input continues, the flow field itself should become antisymmetric in the spanwise direction, but this is not the case.

Figure 6 (b) shows the conditionally-averaged flow field at $t^+ = 100$. These figures demonstrate that the streamwise velocity distribution is drastically modified in the vicinity of the wall, and hence the spatial phase between the control input and the streamwise vortices are also changed, especially around the leg regions of vortices; blowing beneath the streamwise vortices decelerates the flow and shifts the boundary between low and high speed streaks in the spanwise direction. On the other hand, suction beneath the vortices accelerates the flow and shifts the boundary also in the same spanwise direction. The amount of this spanwise shift of the boundary adjacent to the wall depends on the wall elevation of the streamwise vortices, and then the boundary is tilted in the spanwise direction as shown in Fig. 6. And because of this shift, the control input becomes almost 180 degree out-of-phase with the wall-normal velocity induced by the streamwise vortices.

Figure 7 shows the time history of the correlation coefficient of v_w with v at $y^+ = 15.1$. It is observed that the coefficient becomes large negative as the control proceeds and is almost constant at about -0.3. Therefore, the control scheme obtained by the present GA gives similar control input as V-control (Choi *et al*., 1994), although the present scheme requires only the streamwise wall shear stress distribution.

5. CONCLUSIONS

A new practical control scheme of wall turbulence based only on the streamwise wall shear stress was developed with the aid of genetic algorithms and its performance was evaluated using direct numerical simulation of turbulent channel flow. The following conclusions are derived:

1) A simple control scheme, of which the control input is proportional to the spanwise differential of the streamwise wall shear stresses about ± 20 (ν/u_τ) apart in the spanwise direction from the actuator, reduces the wall skin friction as much as 18%.
2) The streaky structures in the vicinity of the wall are drastically altered by the present control. This change enables the present control input to be out of phase with the wall-normal velocity of the near-wall vortices.

REFERENCES

Bewley, T., Choi, H., Temam, R., and Moin, P., 1993, *CTR Annual Research Briefs* 3.

Bewley, T., Moin, P., and Temam, R., 2001, *J. Fluid Mech.*, **447**, 179.

Choi, H., Moin, P., and Kim, J., 1994, *J. Fluid Mech.*, **262**, 75.

Gad-el-Hak, M., 1996, *Appl. Mech. Rev.*, **49**, 365.

Goldberg, D. E., 1989, Genetic Algorithms in Search, Optimization and Machine Learning, Addison-Wesley.

Kasagi, N., Sumitani, Y., Suzuki, Y., and Iida, O., 1995, *Int. J. Heat and Fluid Flow*, **16**, 2.

Kasagi, N., 1998, *Int. J. Heat and Fluid Flow*, **19**, 128.

Kim, J., Moin, P., and Moser, R., 1987, *J. Fluid Mech.*, **177**, 133.

Lee, C., Kim, J., Babcock, D., and Goodman, R., 1997, *Phys. Fluids*, **9**, 1740.

Lee, C., Kim, J., and Choi, H., 1998, *J. Fluid Mech.*, **358**, 245.

Moin, P., and Bewley, T., 1994, *Appl. Mech. Rev.*, **47**, S3.

Robinson, S. K., 1991, *Annu. Rev. Fluid Mech.*, **23**, 601.

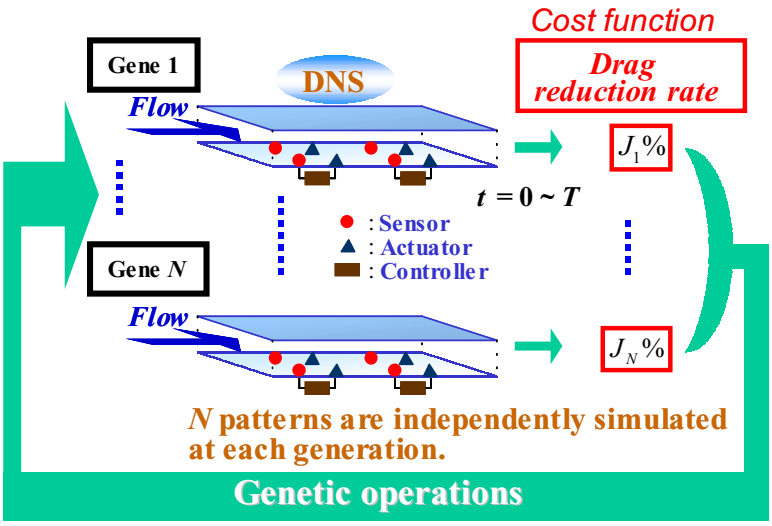

Fig. 1 Schematic diagram of GA-based control.

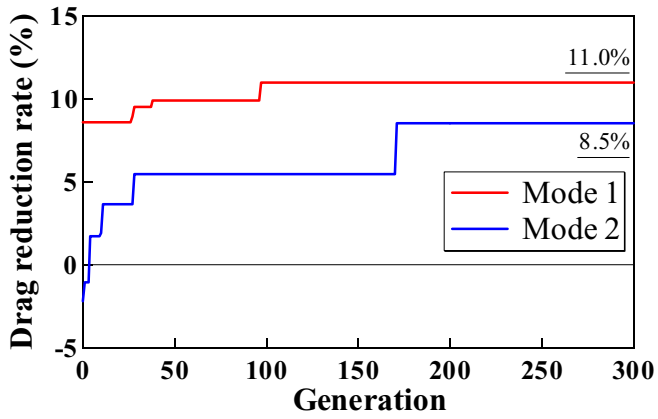

Fig. 2 Evolution of drag reduction rate.

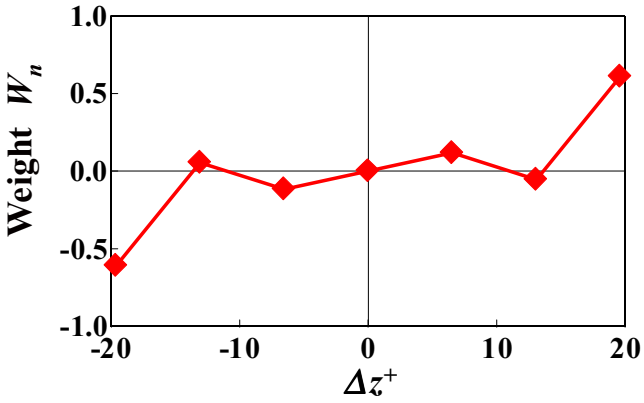

Fig. 3 Weight distribution optimized by GAs.

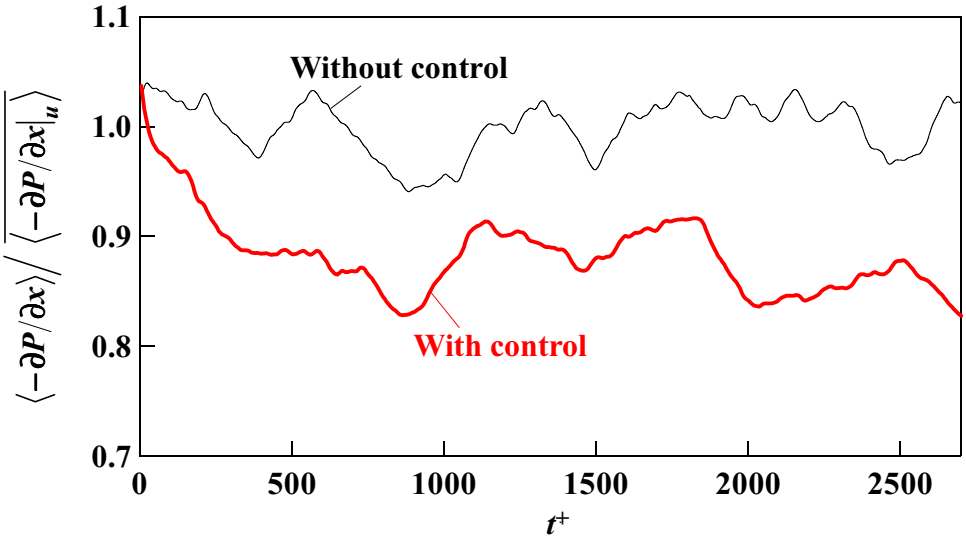

Fig. 4 Time histories of the pressure gradients.

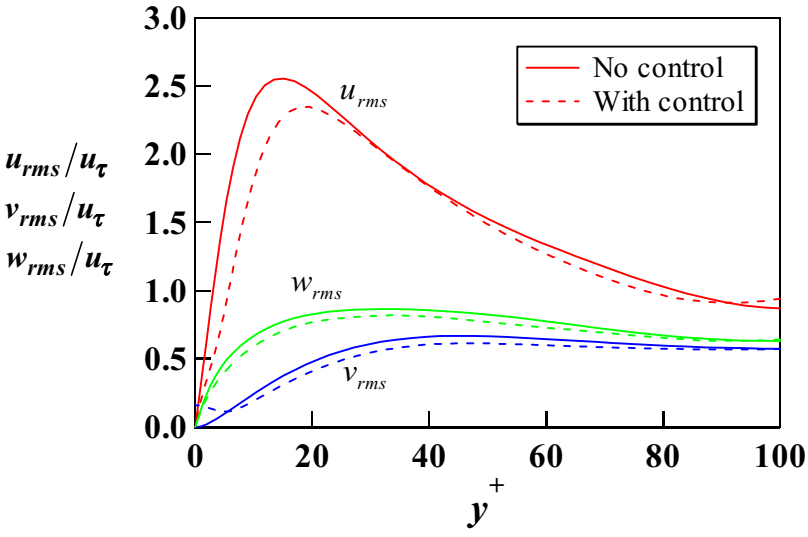

Fig. 5 Root-mean-square velocity fluctuations.

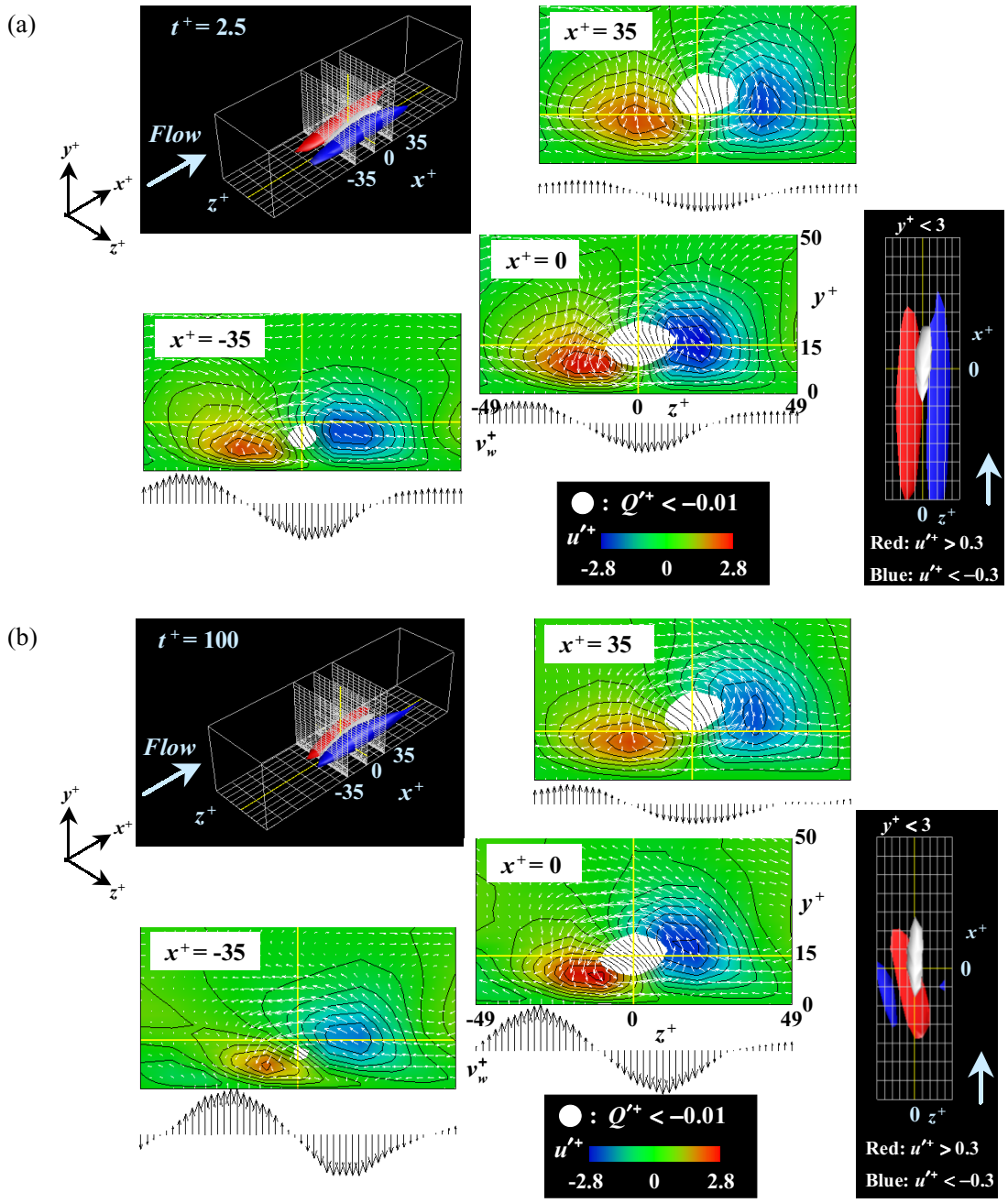

Fig. 6 Conditionally-averaged flow field and control input. Velocity vectors, iso-contours of u'^{+}, and isosurfaces of the second invariant of the deformation tensor (Q^{+} < -0.01): (a) t^{+} = 2.5, (b) t^{+} = 100.

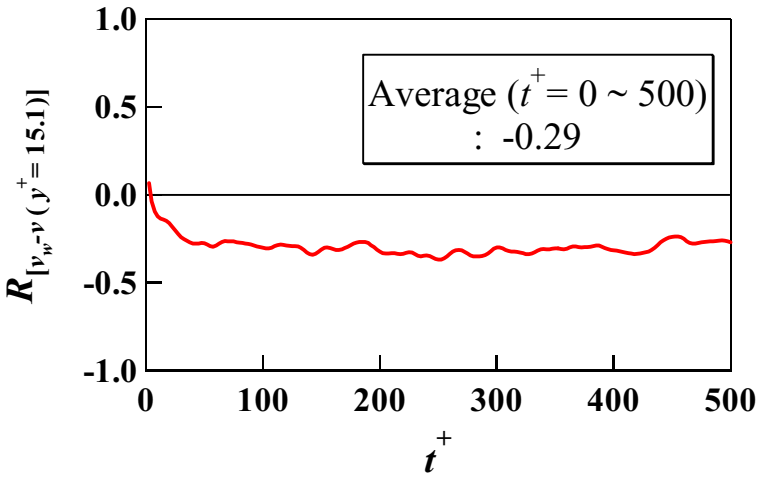

Fig. 7 Time history of the correlation coefficient of v_w with v at y^{+} = 15.1.